



A QSS approach for particle source identification in Tore Supra tokamak

Emmanuel Witrant, Marc Goniche

► To cite this version:

Emmanuel Witrant, Marc Goniche. A QSS approach for particle source identification in Tore Supra tokamak. CDC 2009 - 48th IEEE Conference on Decision and Control, Dec 2009, Shanghai, China. hal-00444549

HAL Id: hal-00444549

<https://hal.science/hal-00444549>

Submitted on 6 Jan 2010

HAL is a multi-disciplinary open access archive for the deposit and dissemination of scientific research documents, whether they are published or not. The documents may come from teaching and research institutions in France or abroad, or from public or private research centers.

L'archive ouverte pluridisciplinaire **HAL**, est destinée au dépôt et à la diffusion de documents scientifiques de niveau recherche, publiés ou non, émanant des établissements d'enseignement et de recherche français ou étrangers, des laboratoires publics ou privés.

A QSS approach for particle source identification in Tore Supra tokamak

Emmanuel WITRANT¹, Marc GONICHE² and *Equipe TORE SUPRA*², September 4, 2009*

Abstract

In this work, we consider the problem of particle source identification from distributed electron density measurements in fusion plasmas, such as the ones obtained in Tore Supra tokamak. A transport model, suitable for identification purposes, is first proposed based on a simplification of classical particle transport models. We then derive a quasi-steady state (QSS) description, which is shown to converge exponentially towards the true solution. Finally, an identification method is proposed based on the QSS model and a shape approximation of the source term. Tore Supra data is used to illustrate the different results with experimental measurements.

1. INTRODUCTION

Recent developments in control theory and controlled thermonuclear fusion research are naturally leading to research topics of common interest that are particularly challenging for both scientific communities. For example, new modeling and identification tools are needed for the understanding and analysis of complex physical phenomena that occur in thermonuclear fusion. The representation (qualitative and quantitative) of particles transport at the plasma edge is an example of such topics.

Tokamak experiments, such as *Tore Supra* or *JET*, are equipped with Lower Hybrid (LH) antennas to heat the plasma and create the toroidal current. The LH waves are recognized as the most efficient non-inductive current drive sources and their use is forecasted for ITER experiment. The efficiency of such antennas is strongly related to our ability to ensure an appropriate coupling between the waves on the plasma, which directly depends on the electron density in a region called the *scrape-off layer* (SOL), located between the last closed magnetic surface (the *separatrix*) and the

wall. This region, as well as the key elements discussed in this paper, are depicted in Fig. 1. The importance of local density control in the SOL is discussed in [1], where dedicated experimental conditions are established for long distance shots (plasma experiments) on Tore Supra. It is further emphasized in [2], where the coupling efficiency is improved thanks to gas puffing in front of the launcher on JET (reduced reflected power). A first attempt to control the coupling between LH and the SOL is proposed in [3], based on a scalar model.

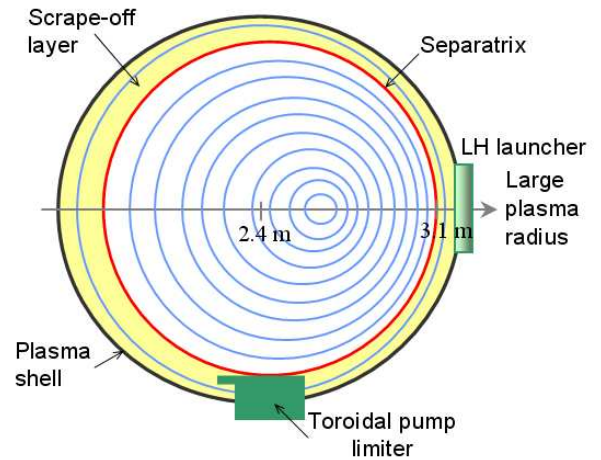


Figure 1. SOL, limiter and LH launcher in a tokamak cross section (i.e. Tore Supra).

The electron density in the SOL is directly influenced by the LH input power P_{LH} [1]. Indeed, a small but significant part of this power is absorbed in the plasma edge during the wave propagation to the core. A possible effect of this absorption is the gas ionization, which results in an increased electron density. This suggests that P_{LH} is a key parameter for the local control of the electron density, and consequently for the coupling efficiency, which motivates the development of new modeling tools based on experimental measurements. On Tore Supra, the electron density is measured by using a microwave reflectometer that has both a good spatial ($r \approx 1$ cm) and temporal resolution ($t \approx 2$ ms for the shot considered).

*The authors are with: ¹ Automatic Control Department, UJF/GIPSA-lab, Grenoble, France, ² Association EURATOM-CEA, CEA/IRFM, Saint Paul Lez Durance, France. The corresponding author email is emmanuel.witrant@gipsa-lab.inpg.fr

The aim of this paper is to develop an identification method for determining the *source term*, i.e. the number of electrons created per unit time and volume, when the high frequency heating is switched on. To achieve this, we derive a particle transport model for the area of non-confined plasma (SOL) and develop an appropriate parametric identification method for distributed systems, based on the reflectometer measurements. The resulting algorithm then provides an efficient tool for analyzing the coupling associated with the electron density in the SOL, even if the detailed physical relationships are unknown.

Our approach is based on a quasi-steady-state (QSS) approximation of the diffusive transport phenomena. The density is considered as the boundary layer while the source term is supposed to have relatively smooth variations. A similar approach has been presented, in the feedback control framework, in [4]. The QSS model is then used to set an optimal shape identification method for the source term. The identification algorithm is validated on a Tore Supra shot that has been specifically set for such research (LH power modulation).

The paper is organized as follows. First, the simplified particle transport dynamics is presented in Section 2, along with some background on classical models. The QSS approximation and the convergence analysis are then detailed in Section 3. Finally, the identification method based on shape estimation is derived in Section 4.

2. SIMPLIFIED TRANSPORT MODEL

The aim of this section is first to present classical models that are used in thermonuclear fusion to determine the particle transport. Thanks to specific hypotheses associated with the physical properties of the SOL, we then propose simplified model that will be used for the particle source identification.

2.1. Energy conservation

The temperature and density behavior are generally set by the transport equation:

$$\frac{3}{2} \frac{\partial nT}{\partial t} = \nabla(n\chi\nabla T) + S_T \quad (1)$$

where $n(x, t)$ is the density, $\chi(x, t)$ is the temperature diffusivity and $S_T(x, t)$ corresponds to heat sources. Various approaches have been proposed for the computation of χ and S_T but their number illustrates the difficulty to model the heat diffusion for tokamak plasmas. Some existing fitting laws provide for the volume average temperature estimation [5] but traditional fitting

curve methods are strongly dependent on the operating conditions.

2.2. Linearized model

If we consider relatively small variations $\tilde{n}(x, t)$ and $\tilde{T}(x, t)$ of the temperature and density around their averaged value $n_0(x)$ and $T_0(x)$, we have that:

$$n(x, t) = n_0(x) + \tilde{n}(x, t), \quad T(x, t) = T_0(x) + \tilde{T}(x, t).$$

The conservation law can then be expressed using the linearized model [6, 7]:

$$\mathcal{A} \frac{\partial}{\partial t} \begin{bmatrix} \tilde{n} \\ \tilde{T} \end{bmatrix} = \begin{bmatrix} S \\ Q \end{bmatrix} u(t) + \mathcal{P} \begin{bmatrix} \tilde{n} \\ \tilde{T} \end{bmatrix} + \nabla \cdot \mathcal{V} \begin{bmatrix} \tilde{n} \\ \tilde{T} \end{bmatrix} + \nabla \cdot \mathcal{D} \nabla \begin{bmatrix} \tilde{n} \\ \tilde{T} \end{bmatrix} \quad (2)$$

where S and Q denote the particle and heat sources,

$$\mathcal{A} = \begin{bmatrix} 1 & 0 \\ \frac{3}{2}T_0 & \frac{3}{2}n_0 \end{bmatrix}, \quad \mathcal{P} = \begin{bmatrix} \frac{\partial S}{\partial n} & \frac{\partial S}{\partial T} \\ \frac{\partial Q}{\partial n} & \frac{\partial Q}{\partial T} \end{bmatrix},$$

$$\mathcal{V} = \begin{bmatrix} \mathcal{V}_{nn} & \mathcal{V}_{nT} \\ \mathcal{V}_{Tn} & \mathcal{V}_{TT} \end{bmatrix}, \quad \mathcal{D} = \begin{bmatrix} \mathcal{D}_{nn} & \mathcal{D}_{nT} \\ \mathcal{D}_{Tn} & \mathcal{D}_{TT} \end{bmatrix},$$

with \mathcal{V}_{ij} and \mathcal{D}_{ij} , $\{i, j\} \in \{n, T\}$ the second order gradients.

2.3. Density behavior in the SOL

In the scrape-off layer, we can simplify the previous model thanks to the following hypotheses:

- the convective effects are neglected, i.e. $\mathcal{V} = 0$;
- the density gradients play a more important role than the temperature gradients in the sink term: $\partial S / \partial T \ll \partial S / \partial n$;
- similarly, we also consider that $\mathcal{D}_{nT} \ll \mathcal{D}_{nn}$;
- the diffusivity term \mathcal{D}_{nn} is constant.

The linearized model (2) is then simplified, for the density dynamics, as:

$$\frac{\partial \tilde{n}}{\partial t} = S u(t) + \frac{\partial S}{\partial n} \tilde{n} + \mathcal{D}_{nn} \frac{\partial^2 \tilde{n}}{\partial r^2}.$$

Considering the static case without sources, the transport coefficients $\partial S / \partial n$ and \mathcal{D}_{nn} can be related to the model proposed in [8]. The final model is described by the dynamics:

$$\frac{\partial \tilde{n}}{\partial t} = D_{\perp}(t) \frac{\partial^2 \tilde{n}}{\partial r^2} - \frac{c_s(r, t)}{2L_c(r, t)} \tilde{n} + S(r, t) \quad (3)$$

where D_{\perp} is the cross-field diffusion coefficient (typically $\sim 1 \text{ m}^2 \text{ s}^{-1}$), c_s is the sound speed, L_c is the connecting length along the flux tube to the flow stagnation point and $S = S_l + S_{LH}$ reflects the particle source induced by the limiter S_l and the LH antenna S_{LH} . The sound speed can be approximated as $c_s \approx \sqrt{(T_e + T_i)/m_i}$, where T_e and T_i are the electron and ion temperatures, and m_i is the ion mass. The ratio T_i/T_e is obtained thanks to the experimental measurements described in [9]. L_c is deduced from the safety factor q (which typically varies by 10 % in the SOL) as $L_c = 2\pi r q$.

A Neumann boundary condition $\partial \tilde{n}(0, t)/\partial r = 0$ is set close to the center while a Dirichlet one $\tilde{n}(L, t) = \tilde{n}_L(t)$, where $\tilde{n}_L(t)$ is given by the measurements, governs the plasma edge. Note that $r = 0, L$ denote relative coordinates with respect to the model domain of validity (i.e. $r = 0$ at the separatrix location). The data set considered in this paper is characterized by repeated LH impulses, which highlight the impact of LH antenna.

2.4. Problem statement

The problem considered in this paper is to determine $S(r, t)$ in (3) from the given signals of $n(r, t)$. The transport parameters (supposed constant according to the quasi-steady state behavior described in the next section) D_{\perp} , c_s and L_c are obtained from existing models and measurements.

3. QUASI-STEADY STATE BEHAVIOR

The model (3) belongs to a more general class of transport systems that involves diffusion, mass losses and a distributed source. We suppose that averaged values of diffusion and sink terms can provide for a good enough approximation. Taking into account the fact that we are interested in the averaged impact of the source term, its time-scale is denoted by t' . Using the subscripts t and x to denote the time and space derivatives, respectively, where $x = r/L \in [0, 1]$ is the normalized radius, the class of systems considered can be described as:

$$\begin{cases} \tilde{n}_t(x, t) = \alpha \tilde{n}_{xx}(x, t) - \gamma(t') \tilde{n}(x, t) + S(x, t'), \\ \tilde{n}_x(0, t) = 0, \quad \tilde{n}(1, t) = \tilde{n}_L(t), \\ \tilde{n}(x, 0) = \tilde{n}_{r0}, \end{cases} \quad (4)$$

where $\alpha = D_{\perp}/L^2$ is the diffusion, $\gamma = \overline{c_s}/(2\overline{L_c}) > 0$ is the sink term and $\overline{A}(t) \doteq \int_0^L A(x, t) dx$.

In this section, we investigate the transport model's properties along the lines suggested in [4] in a control design framework. More precisely, we suppose *slow variations* on the time-scale of the input t' to determine

the quasi-steady state behavior of (4). It is then shown that the true model converges exponentially towards its equilibrium value.

3.1. Quasi-steady state (QSS) solution

In order to find the QSS of (4), we consider the variables in the time-scale t' as constant and determine the steady-state behavior of \tilde{n} . The model considered consequently writes as:

$$\begin{cases} \alpha \tilde{n}_{e,xx} - \gamma \tilde{n}_e + S = 0, \\ \tilde{n}_{e,x}(0, t) = 0, \quad \tilde{n}_e(1, t) = \tilde{n}_L(t'). \end{cases} \quad (5)$$

The homogeneous solution \tilde{n}_{e_h} is determined by setting $S = 0$, which implies the solution:

$$\tilde{n}_{e_h}(x, t') = k_1(t') \cosh \lambda x + k_2(t') \sinh \lambda x,$$

with $\lambda(t') \doteq \sqrt{\gamma/\alpha}$. Applying the boundary conditions to the previous equation, the constant coefficients are $k_1(t') = \tilde{n}_L(t')/\cosh \lambda$ and $k_2(t') = 0$. Note that this homogeneous solution can be used to compute the density profile $n_0(x)$ based on averaged experimental measurements of the boundary conditions.

The distributed source is taken into account thanks to the *variation of parameters* method (created by Lagrange and available in classical textbooks, such as [10]) by considering the set of solutions:

$$\tilde{n}_{e_{nh}}(x, t') = u_1(x, t') \cosh \lambda x + u_2(x, t') \sinh \lambda x.$$

The non-homogenous solution is obtained as follows. Substituting the previous equation into (5) and assuming that

$$\begin{aligned} 0 &= \frac{\partial u_1}{\partial x} \cosh \lambda x + \frac{\partial u_2}{\partial x} \sinh \lambda x, \\ -\frac{1}{\sqrt{\alpha\gamma}} S &= \frac{\partial u_1}{\partial x} \sinh \lambda x + \frac{\partial u_2}{\partial x} \cosh \lambda x, \end{aligned}$$

with the previous definition of λ , then u_1 and u_2 are given as

$$\begin{aligned} u_1(x, t') &= \frac{1}{\sqrt{\alpha\gamma}} \int_0^x \sinh(\lambda\eta) S(\eta, t') d\eta, \\ u_2(x, t') &= -\frac{1}{\sqrt{\alpha\gamma}} \int_0^x \cosh(\lambda\eta) S(\eta, t') d\eta. \end{aligned}$$

We then obtain:

$$\tilde{n}_{e_{nh}}(x, t') = \frac{1}{\sqrt{\alpha\gamma}} \int_0^x \sinh[\lambda(\eta - x)] S(\eta, t') d\eta.$$

Solving for the boundary conditions, the QSS behavior is finally given by:

$$\tilde{n}_{e_{qss}}(x, t') = \frac{\tilde{n}_L - C(S)}{\cosh \lambda} \cosh \lambda x + \frac{1}{\sqrt{\alpha\gamma}} \int_0^x \sinh[\lambda(\eta - x)] S(\eta, t') d\eta, \quad (6)$$

$$\text{with } C(S) \doteq \frac{1}{\sqrt{\alpha\gamma}} \int_0^1 \sinh[\lambda(\eta - 1)] S(\eta, t') d\eta.$$

3.2. Convergence properties

In this section, we investigate the convergence of the actual model (4) towards the QSS approximation (6). Defining the difference between the model and its approximation as:

$$z(x, t) \doteq \tilde{n}(x, t) - \tilde{n}_e(x, t),$$

the dynamics of z is directly given by:

$$\begin{cases} z_t = \alpha z_{xx} - \gamma z, \\ z_x(0, t) = z(1, t) = 0. \end{cases}$$

Convergence properties and PDE stability conditions are particularly difficult to establish directly. Instead, the use of norms may greatly simplify the problem and allows for the definition of specific criteria [4]. In this analysis, we consider the convergence analysis in the \mathcal{L}_2 sense, with the Lyapunov functional (or \mathcal{L}_2 norm):

$$\mathcal{L}(t) = \frac{1}{2} \int_0^1 z(x, t)^2 dx.$$

Its dynamics is derived as:

$$\begin{aligned} \frac{d}{dt} \mathcal{L}(t) &= \int_0^1 z z_t dx = \alpha \int_0^1 z z_{xx} dx - \gamma \int_0^1 z^2 dx \\ &= -\alpha \int_0^1 z_x^2 dx - \gamma \int_0^1 z^2 dx \\ &\leq -\frac{\alpha}{4} \int_0^1 z^2 dx - \gamma \int_0^1 z^2 dx = -\frac{\alpha + 4\gamma}{2} \mathcal{L}(t), \end{aligned}$$

where the third equality is obtained by applying integration by part ($(z_x z)_x = z_{xx} z + z_x^2$) and from the boundary conditions, and the inequality comes from the application of Poincaré's inequality ($\int_0^1 f(x)^2 dx \leq 2f(0)^2 + 4 \int_0^1 f_x(x)^2 dx$). As a direct consequence:

$$\mathcal{L}(t) \leq e^{-\frac{\alpha+4\gamma}{2}t} \mathcal{L}(0),$$

or, equivalently in terms of the convergence error:

$$\|z(x, t)\|_2^2 \leq e^{-\frac{\alpha+4\gamma}{2}t} \|z(x, 0)\|_2^2.$$

The transport model then converges exponentially towards the QSS approximation (6) if $\alpha + 4\gamma > 0$ (which is the case for the particles transport since α and γ are positive), at a rate $(\alpha + 4\gamma)/2$. In order to verify the QSS approximation, the time constant associated with the source dynamics τ_S has to verify the constraint:

$$\tau_S \gg \frac{2}{\alpha + 4\gamma} = \frac{2L^2 \overline{L_C}}{D_1 \overline{L_C} + 2L^2 \overline{c_s}}. \quad (7)$$

For the data considered, we obtain $\tau_S \gg 10.3 \text{ ms}$. The data sampling time being 2 ms , τ_S is an important parameter to take into consideration when estimating the source term.

4. IDENTIFICATION OF THE SOURCE TERM

Supposing a given shape for the source term, a parametric identification method is established in this section to determine the parameter set from experimental data and the QSS model.

4.1. Shape estimation

As an approximation, the source term is considered as the sum of two curves (limiter and LH sources) determined from the QSS description. Our analysis is restricted to the functions described as:

$$S(x, t') \approx \sum_{i=l, LH} \vartheta_i(t') e^{\beta(x, \mu_i(t'), \sigma_i(t'))},$$

where l and LH denote the limiter and the LH source, respectively, ϑ_i sets the amplitude, $\beta(\cdot)$ is the dilatation function, σ_i a dilatation coefficient and μ_i the translation. Note that this family of curves could easily be extended to sigmoids or splines. A similar approach was used in [11], to obtain an approximation of temperature profiles in a current density model. The set of parameters $\theta(t') \doteq \{\vartheta_l, \mu_l, \sigma_l, \vartheta_{LH}, \mu_{LH}, \sigma_{LH}\}$ is obtained by solving the least squares problem:

$$\min_{\theta} \left\{ J(\theta, t') = \frac{1}{2} \int_0^1 (\tilde{n}_{em}(x, t') - \tilde{n}_{e_{qss}}(x, \theta, t'))^2 dx \right\}$$

for each sampling instant t' , using the experimental measurements \tilde{n}_{em} and with boundary constraints on θ given by the physical properties of the system. This is done thanks to *Matlab*[®] function `fmincon`, a subspace trust-region method based on the interior-reflective Newton method described in [12, 13]. Similar gradient-based methods can be used, with the constraint that they apply to large-scale nonlinear systems. The

gradient and pseudo-Hessian (Gauss-Newton approximation) are obtained, respectively, as:

$$\begin{aligned}\nabla_{\theta} J(\theta, t') &= - \int_0^1 S_{\theta}(x, t') (\tilde{n}_{e_m} - \tilde{n}_{e_{qss}}) dx, \\ \Psi_{\theta} J(\theta, t') &= \int_0^1 S_{\theta}(x, t') S_{\theta}(x, t')^T dx,\end{aligned}$$

where $S_{\theta} \doteq \partial \tilde{n}_{e_{qss}} / \partial \theta$ is the sensitivity of $\tilde{n}_{e_{qss}}$ with respect to θ . The sensitivity function is derived as:

$$\begin{aligned}S_{\theta} &= \frac{-\cosh \lambda x}{\sqrt{\alpha \gamma} \cosh \lambda} \int_0^1 \sinh[\lambda(\eta - 1)] \frac{\partial S(\eta, t')}{\partial \theta} (1, t') d\eta \\ &+ \frac{1}{\sqrt{\alpha \gamma}} \int_0^x \sinh[\lambda(\eta - x)] \frac{\partial S(\eta, t')}{\partial \theta} (\eta, t') d\eta,\end{aligned}$$

with (applying the chain rule):

$$\begin{aligned}\frac{\partial S}{\partial \theta} &= \left[\frac{\partial S}{\partial \vartheta_i}; \frac{\partial S}{\partial \mu_i}; \frac{\partial S}{\partial \sigma_i}; \frac{\partial S}{\partial \vartheta_{LH}}; \frac{\partial S}{\partial \mu_{LH}}; \frac{\partial S}{\partial \sigma_{LH}} \right], \\ \frac{\partial S}{\partial \vartheta_i}(x, t') &= e^{\beta(x, \mu_i(t'), \sigma_i(t'))}, \\ \frac{\partial S}{\partial \mu_i}(x, t') &= \vartheta_i(t') \frac{\partial S}{\partial \vartheta_i}(x, t') \frac{\partial \beta}{\partial \mu_i}(x, t'), \\ \frac{\partial S}{\partial \sigma_i}(x, t') &= \vartheta_i(t') \frac{\partial S}{\partial \vartheta_i}(x, t') \frac{\partial \beta}{\partial \sigma_i}(x, t').\end{aligned}$$

In order to fulfill the constraint on the source dynamics, the resulting optimal set of parameters θ^* is smoothed using the *nearly equal ripple approximation* proposed in [14] with a passband edge much smaller than $(\alpha + 4\gamma)/2$, to satisfy the QSS condition (7).

4.2. Example: Gaussian fit

The results presented in the previous section are illustrated by considering the source term as a sum of Gaussian distributions:

$$S(x, t') \approx \sum_{i=l, LH} \vartheta_i(t') e^{-(\mu_i(t') - x)^2 / 2\sigma_i(t')}. \quad (8)$$

The optimal set of parameters θ^* is obtained using:

$$\begin{aligned}\beta(x, \mu_i(t'), \sigma_i(t')) &= -\frac{(\mu_i(t') - x)^2}{2\sigma_i(t')}, \\ \frac{\partial S}{\partial \vartheta_i}(x, t') &= e^{-(\mu_i(t') - x)^2 / 2\sigma_i(t')}, \\ \frac{\partial \beta}{\partial \mu_i}(x, t') &= \frac{x - \mu_i(t')}{\sigma_i(t')}, \\ \frac{\partial \beta}{\partial \sigma_i}(x, t') &= \frac{(\mu_i(t') - x)^2}{2\sigma_i^2(t')} = \frac{1}{2} \left(\frac{\partial \beta}{\partial \mu_i}(x, t') \right)^2.\end{aligned}$$

The time evolution of the resulting Gaussian param-

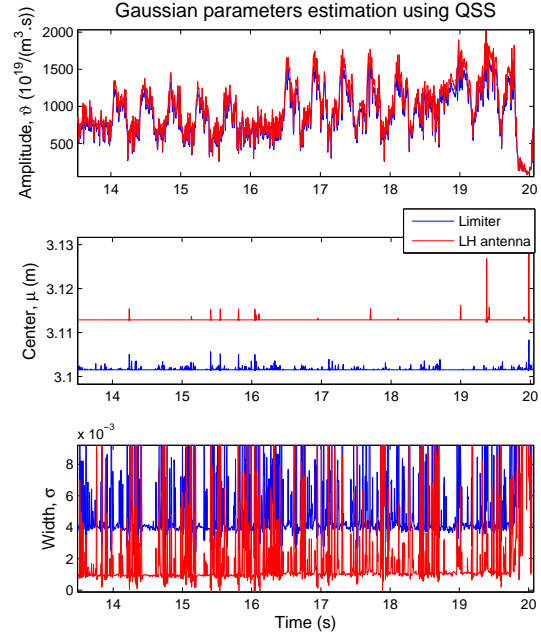


Figure 2. Shape parameters for the Gaussian approximation.

eters is presented in Fig. 2. We can see that the source locations are clearly distinct, with a wider source closer to the plasma center that is due to the limiter. The amplitudes illustrate properly the LH impulses, with peaks corresponding to their time location, but are clearly correlated. This may motivate further investigation on the chosen optimal algorithm that may give only a suboptimal result, due to the system nonlinearities. Note also that the standard deviation is very tight, resulting in a high amplitude of ϑ_i . Finally, the Gaussian parameters are strongly related to the transport coefficients (i.e. increasing γ results in an increased σ_i and a decreased ϑ_i), which may be considered as optimized parameters to decrease the estimation error.

The source term is introduced in the QSS model (6) and compared with the experimental data on Fig. 3. We can see that the estimation error is acceptable in the region between 3.11 and 3.15 m, which corresponds approximately to the domain of validity of the model. Indeed, we may cross the separatrix when going closer to the center and the plasma shell at the edge may act as a particle source not considered explicitly. Note that the “accurate region” (where the error is less than 10%) is increased after 16.5 s. This may be correlated with the higher amplitude of the source and imply that the transport coefficients values are an important source of error, as their relative importance is consequently re-

duced. Unfiltered data have been used for the source determination: the proposed approach is then relatively robust to measurement noise. Finally, the LH modulations do not create a significant associated error, which confirms that our approach is suited for their analysis as a source term.

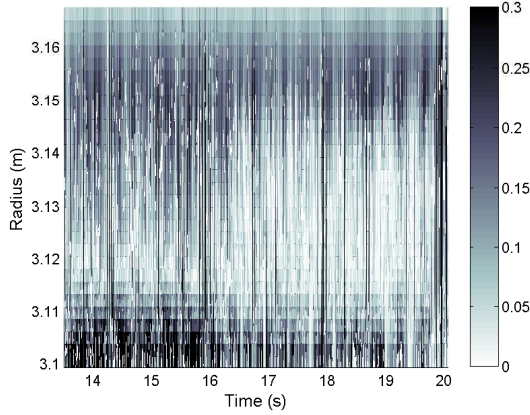


Figure 3. Comparison of the $\tilde{n}_{eqs}(x, t)$ with the experimental data (normalized error).

5. CONCLUSIONS

In this work we considered the problem of particle source identification in the scrape-off layer from distributed measurements, which is a topic of main importance in the field of controlled thermonuclear fusion. Based on existing physical models, we proposed a simplified one that implies diffusive transport and a sink term, additionally to the source term. A QSS model was derived and proven to converge exponentially towards the exact solution of the dynamic model. A parametric identification method based on least squares approximation and the QSS model was proposed, supposing a given shape for the source term. The accuracy of the final model was discussed based on experimental measurements and shown to validate specific model properties.

References

- [1] J. Mailloux, M. Goniche, P. Bibet, P. Froissard, C. Grisolia, R. Guirlet, and J. Gunn, “Long distance coupling of the lower hybrid waves on Tore Supra,” in *Proc. of the 25th European conference on Cont. Fus. and Plasma heating*, E. P. Society, Ed., vol. 23, no. I, Prague, 1998, p. 1394.
- [2] A. Ekedahl, G. Granucci, J. Mailloux, Y. Baranov, S. Erents, E. Joffrin, X. Litaudon, A. Loarte, P. Lo-
mas, D. McDonald, V. Petrzilka, K. Rantamäki, F. Rimini, C. Silva, A. Stamp, M. Tuccillo, and JET EFDA Contributors, “Long distance coupling of lower hybrid waves in JET plasmas with edge and core transport barriers,” *Nucl. Fusion*, vol. 45, no. 5, pp. 351–359, 2005.
- [3] D. Carnevale, L. Zaccarian, A. Astolfi, and S. Podda, “Extremum seeking without external dithering and its application to plasma RF heating on FTU,” in *IEEE Conference on Decision and Control*, Cancun, Mexico, Dec. 2008.
- [4] R. Vazquez and M. Krstic, *Control of Turbulent and Magnetohydrodynamic Channel Flows: Boundary Stabilization and State Estimation*, ser. Systems & Control: Foundations & Applications. Springer - Birkhäuser, 2008.
- [5] ITER Physics Expert Groups, “Chapter 2: Plasma confinement and transport,” *Nucl. Fusion*, vol. 39, no. 12, pp. 2175–2249, 1999.
- [6] K. Gentle, “Dependence of heat pulse propagation on transport mechanisms: Consequences of nonconstant transport coefficients,” *Phys. Fluids*, vol. 31, p. 1105, 1988.
- [7] J. Moret and Equipe Tore Supra, “Tokamak transport phenomenology and plasma dynamic response,” *Nucl. Fusion*, vol. 32, no. 7, pp. 1241–1258, 1992.
- [8] J. Wesson, *Tokamaks*, 2nd ed., ser. Oxford engineering science. New York: Oxford Science Publications, 1997, no. 48.
- [9] M. Kočan, J. Gunn, J.-Y. Pascal, G. Bonhomme, C. Fenzi, E. Gauthier, and J.-L. Segui, “Edge ion-to-electron temperature ratio in the Tore Supra tokamak,” *Plasma Phys. Control. Fusion*, vol. 50, pp. 125 009–125 019, 2008.
- [10] W. Boyce and R. DiPrima, *Elementary differential equations and boundary value problems*, 6th ed. John Wiley & Sons, 1997.
- [11] E. Witrant, E. Joffrin, S. Brémond, G. Giruzzi, D. Mazon, O. Barana, and M. P., “A control-oriented model of the current profile in tokamak plasma,” *Plasma Phys. Control. Fusion*, vol. 49, pp. 1075–1105, 2007.
- [12] T. Coleman and Y. Li, “On the convergence of reflective Newton methods for large-scale nonlinear minimization subject to bounds,” *Mathematical Programming*, vol. 67, no. 2, pp. 189–224, 1994.
- [13] —, “An interior, trust region approach for nonlinear minimization subject to bounds,” *SIAM Journal on Optimization*, vol. 6, pp. 418–445, 1996.
- [14] J. Kaiser and W. Reed, “Data smoothing using low-pass digital filters,” *Review of Scientific Instruments*, vol. 48, no. 11, pp. 1447–1457, Nov. 1977.